

IDENTIFICATION OF TARGET IMAGE REGIONS BASED ON BIFURCATIONS OF A FIXED POINT IN A DISCRETE-TIME OSCILLATOR NETWORK

KEN'ICHI FUJIMOTO¹, MIO KOBAYASHI², TETSUYA YOSHINAGA¹
AND KAZUYUKI AIHARA³

¹Institute of Health Biosciences
The University of Tokushima

3-18-15 Kuramoto, Tokushima 770-8509, Japan
{ fujimoto; yosinaga }@medsci.tokushima-u.ac.jp

²Department of Systems and Control Engineering
Anan National College of Technology
265 Aoki Minobayashi-cho, Anan 774-0017, Japan
kobayashi@anan-nct.ac.jp

³Institute of Industrial Science
The University of Tokyo
4-6-1 Komaba, Meguro-ku, Tokyo 153-8505, Japan
aihara@sat.t.u-tokyo.ac.jp

Received November 2011; revised April 2012

ABSTRACT. *Image segmentation is a fundamental technique in image processing. We call the function that extracts blobs (image regions) in a given image and exhibits them in a time series “dynamic image segmentation”. It is known that a locally excitatory globally inhibitory oscillator network (LEGION) described by ordinary differential equations is an interesting dynamic image-segmentation system using synchronization of coupled oscillators. On the other hand, we developed a discrete-time oscillator network that can perform dynamic image segmentation by synchronizing the oscillatory responses that are formed by periodic points in dynamics of discrete-time oscillators. Compared with LEGION, the proposed system can significantly reduce a computational cost because it does not need unnecessary numerical integration; moreover, we can design the suitable values of the system parameters for dynamic image segmentation on the basis of analyzed results on bifurcations of fixed and periodic points. In this paper, we describe how the topological property of a fixed point corresponding to non-oscillatory responses that are unsuitable for dynamic image segmentation in the proposed system gives significant information on the structure of regions in a given binary (black and white) image. We also suggest a novel way to identify the number of image regions without performing a segmentation process.*

Keywords: Discrete-time oscillator, Fixed point, Neimark-Sacker bifurcation, Dynamic image segmentation, The number of image regions

1. **Introduction.** The dynamics of coupled oscillators has been paid much attention in many fields such as physics, chemistry, engineering, and neuroscience [1, 2, 3, 4]. According to the coupling structure of oscillators and the dynamical properties of each individual oscillator, coupled oscillators produce various characteristics as fully incoherent, partially coherent, and fully coherent states. Synchronization [1] that generates a coherent state is a remarkable phenomenon and has been studied for various oscillator models [2, 3, 4].

Synchronization of coupled oscillators can be applied to image segmentation [5, 6, 7]. Image segmentation is a fundamental technique in image processing. The problem with

image segmentation is still serious and various frameworks have been proposed to solve this problem [8, 9, 10]. For example, the k -means method [11] is well known as an image-segmentation method for gray-level images. However, as prior information of a segmentation process, it requires the number of image regions to be segmented in a given image. The number is determined by users and is often given as the number of gray levels to be segmented. In contrast, as a novel image-segmentation system using coupled oscillators, a locally excitatory globally inhibitory oscillator network (LEGION) [5, 6] has been proposed.

A LEGION is composed of an inhibitor and the same number of oscillators as that of pixels in a given image. The dynamics of a LEGION is described by ordinary differential equations. Using in-phase and out-of-phase synchronization of oscillators, a LEGION can extract blobs (image regions) in a given image and can exhibit them in a time series. We call this function “dynamic image segmentation”. Thus a LEGION provides remarkable image segmentation without the prior information on the number of image regions. However, numerical integration with a high computational cost such as LSODE [12] is needed to accurately calculate the behavior of a LEGION, the number of image regions to be segmented in a segmentation process is limited from the nature of oscillators, and we cannot systematically tune system parameter values so that dynamic image segmentation is properly performed because it is difficult to analyze bifurcations of equilibria and periodic oscillations in a LEGION.

On the other hand, we developed a discrete-time oscillator network [13] that can perform dynamic image segmentation. The dynamics of the proposed oscillator that is modified on the basis of a chaotic neuron model [14] is described by a two-dimensional discrete-time map. Our oscillators can generate oscillatory responses that are formed by periodic points like relaxation oscillations observed in continuous-time dynamical systems. The proposed oscillator network consists of a global inhibitor and the discrete-time oscillators arranged in a grid so that each discrete-time oscillator corresponds to a pixel in a given image. Dynamics of the global inhibitor is also described by a discrete-time map. According to the synchronization of the oscillatory responses of discrete-time oscillators, our oscillator network can perform dynamic image segmentation without the prior information on the number of image regions like a LEGION. Moreover, the proposed system can significantly reduce a computational cost to work compared with that of a LEGION because numerical integration is unnecessary. The type of a periodic point that appears in a steady state determines the feasibility of dynamic image segmentation. The appearance depends on parameter values, so we tuned parameter values for dynamic image segmentation based on the results of bifurcation analysis for periodic points and a fixed point in reduced models of our systems [15, 16, 17]. It is also an advantage over a LEGION that we can tune parameter values on the basis of such analyzed results.

The proposed system, however, has a limitation with respect to the number of image regions to be segmented. To solve this, Musashi et al. [18] have proposed a successive algorithm of dynamic image segmentation for a given image with the large number of image regions. To briefly explain the algorithm, images segmented with our dynamic image-segmentation system are represented as inner nodes in a hierarchical tree structure in which the root node corresponds to a given (the original) image with a large number of image regions. Dynamic image segmentation is successively performed for respective images corresponding to inner nodes. After that it becomes a leaf node if an image corresponding to an inner node has only one image region, i.e., the successive algorithm terminates when the tree is complete. Therefore, it is significant and useful to identify the number of image regions before segmentation processes for pruning useless dynamic image-segmentation processes in the successive algorithm.

In this paper, we describe how the topological property of a fixed point, which corresponds to non-oscillatory responses and is unsuitable for dynamic image segmentation, gives significant information on the structure of regions in a given binary (black and white) image. In other words, by computing the characteristic multipliers of a fixed point when it bifurcates, we can identify the number of image regions and background pixels. This fact is not only informative in image segmentation but also interesting from the viewpoint of bifurcation theory.

2. Dynamic Image Segmentation System. Figure 1 shows the architecture of our discrete-time oscillator network for dynamic image segmentation [13]. It consists of a global inhibitor and N discrete-time oscillators arranged in a grid so that each one corresponds to a pixel in an N -pixel input image. Couplings between neighboring oscillators and self-feedback connections are formed depending on the feature values of pixels in a given input image as described below.

A discrete-time oscillator has two internal variables, and the dynamics of the i th discrete-time oscillator is defined by

$$x_i(t+1) = k_f x_i(t) + d_i - W_z g(z(t), \theta_z) + \frac{W_x}{M_i} \sum_{j \in L_i} g(x_j(t) + y_j(t), \theta_c) \quad (1)$$

$$y_i(t+1) = k_r y_i(t) - \alpha g(x_i(t) + y_i(t), \theta_c) + a. \quad (2)$$

Here, $t \in \mathbb{Z}$ denotes the discrete time, and d_i represents the direct current input with a value set by the feature value of the i th pixel in an input image. We used pixel values as feature values. Oscillators corresponding to pixels with only a high d_i value have self-feedback connections, and connections with neighboring oscillators (DO_i and DO_j) are formed only if $d_i \simeq d_j$. Thus oscillators with self-feedback connections can generate oscillatory responses. The third and fourth terms on the right side of (1) correspond to suppressive input from a global inhibitor and excitatory input from neighboring oscillators, including itself. W_z and W_x denote coupling strength from a global inhibitor to the i th oscillator and that from a neighboring oscillator to the i th oscillator, respectively; L_i and M_i correspond to the set of the i th oscillator and its four neighboring ones and the number

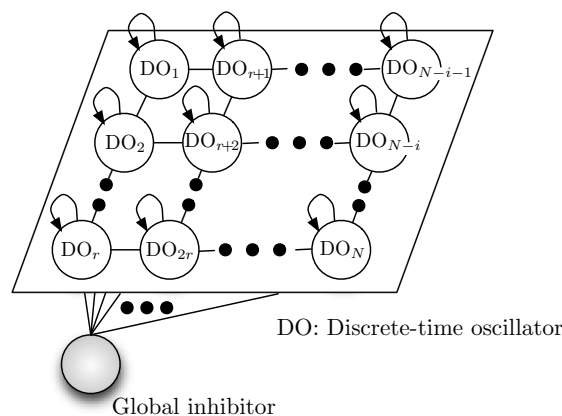


FIGURE 1. Architecture of proposed discrete-time oscillator network

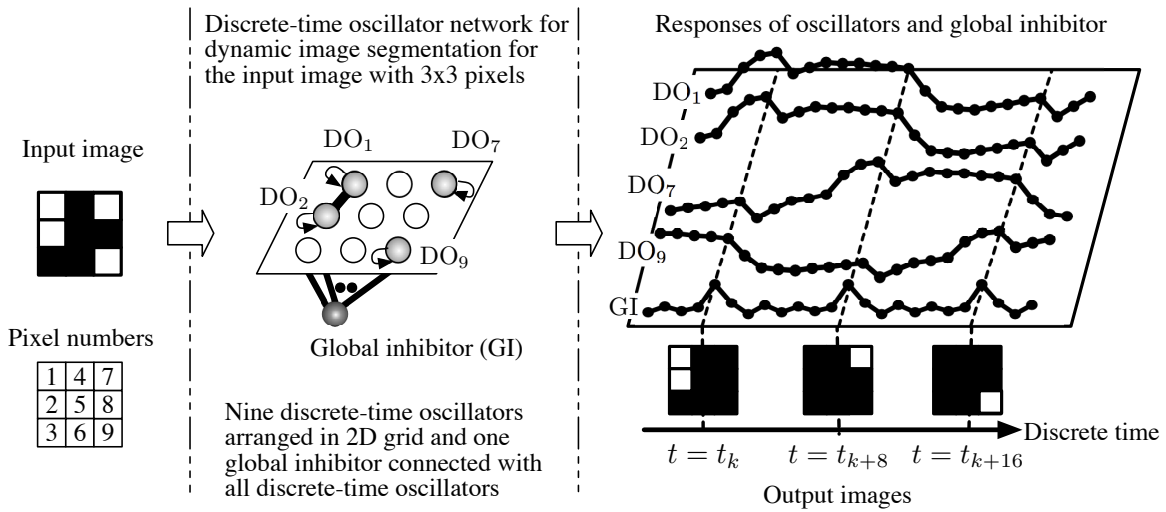


FIGURE 2. Scheme of dynamic image segmentation using our proposed system

of elements in L_i . The dynamics of the global inhibitor is defined as

$$z(t + 1) = \phi \left\{ g \left(\sum_{k=1}^N g(x_k(t) + y_k(t), \theta_f), \theta_d \right) - z(t) \right\}, \quad (3)$$

so that it can detect one or more oscillators with a higher activity level than that of the threshold parameter θ_f and can output a spike simultaneously. $g(\cdot, \cdot)$ in (1)-(3) represents the output function of an oscillator or a global inhibitor and is defined by

$$g(u, \theta) = \frac{1}{1 + \exp(-(u - \theta)/\varepsilon)}. \quad (4)$$

In (1)-(4), $k_f, d_i, W_z, \theta_z, W_x, \theta_c, k_r, \alpha, a, \phi, \theta_f, \theta_d$, and ε are system parameters.

Let us illustrate the behavior of our system and the scheme of dynamic image segmentation for a binary (black and white) image in Figure 2. We set the values of d_i s to the same high values for oscillators corresponding to white pixels and set those in the other oscillators to zero. In Figure 2, the 1st, 2nd, 7th, and 9th oscillators have self-feedback connections, and the excitatory coupling between the 1st and 2nd oscillators is also formed. Oscillators corresponding to only white pixels can generate oscillatory responses corresponding to periodic points. Also, oscillatory responses of the first and second oscillators can be synchronized because of the excitatory coupling. The global inhibitor is connected to all the oscillators and suppresses their activity levels when one or more oscillators have high activity levels. This causes synchronized responses in directly coupled oscillators and out-of-phase responses in uncoupled ones. Associating the amplitude value of the i th oscillator with the i th pixel value at every discrete time enables the segmented images to be output and exhibited as a time series. This is how our system works as a dynamic image-segmentation system.

3. Fixed Point and Its Bifurcation. Let $\mathbf{x}(t) = (x_1(t), y_1(t), \dots, x_N(t), y_N(t), z(t))^T \in \mathbb{R}^S$, where $S = 2N + 1$. \top denotes the transpose of a vector. The dynamics of our discrete-time dynamical system for an N -pixel image is described as

$$\mathbf{x}(t + 1) = \mathbf{f}(\mathbf{x}(t)), \quad (5)$$

and equivalently, its iterated map is defined by

$$\mathbf{f} : \mathbb{R}^S \rightarrow \mathbb{R}^S; \quad \mathbf{x} \mapsto \mathbf{f}(\mathbf{x}), \tag{6}$$

where the nonlinear function $\mathbf{f} = (f_1, f_2, \dots, f_S)^\top$ is described as

$$\mathbf{f} = \begin{pmatrix} k_f x_1 + d_1 - W_z g(z, \theta_z) + \frac{W_x}{M_1} \sum_{j \in L_1} g(x_j + y_j, \theta_c) \\ k_r y_1 - \alpha g(x_1 + y_1, \theta_c) + a \\ \vdots \\ k_f x_N + d_n - W_z g(z, \theta_z) + \frac{W_x}{M_N} \sum_{j \in L_N} g(x_j + y_j, \theta_c) \\ k_r y_N - \alpha g(x_n + y_n, \theta_c) + a \\ \phi \left\{ g \left(\sum_{k=1}^N g(x_k + y_k, \theta_f), \theta_d \right) - z \right\} \end{pmatrix}. \tag{7}$$

Next, let us define the fixed point and its characteristic multiplier. A point $\mathbf{x}^* \in \mathbb{R}^S$ satisfying

$$\mathbf{x}^* - \mathbf{f}(\mathbf{x}^*) = \mathbf{0} \tag{8}$$

becomes a fixed point of \mathbf{f} . The characteristic equation of \mathbf{x}^* is defined by

$$\chi(\mathbf{x}^*, \mu) = \det(\mu \mathbf{E} - D\mathbf{f}(\mathbf{x}^*)) = 0, \tag{9}$$

where \mathbf{E} , $D\mathbf{f}(\mathbf{x}^*)$, and $\mu \in \mathbb{C}$ correspond to the $S \times S$ identity matrix, the Jacobian matrix of \mathbf{f} at $\mathbf{x} = \mathbf{x}^*$, and one of the S characteristic multipliers for \mathbf{x}^* . Note that all the elements of $D\mathbf{f}(\mathbf{x}^*)$ can be analytically computed.

The topological property of a fixed point is determined on the basis of the arrangement of all characteristic multipliers. When one or more characteristic multipliers of a fixed point are on the circumference of a unit circle in the complex plane, the topological property of the fixed point is changed, and then a bifurcation occurs. For example, a Neimark-Sacker bifurcation occurs if one or more pairs of complex-conjugate characteristic multipliers are on the circumference. Kawakami [19] has classified the bifurcation types and has proposed a method to compute bifurcation points.

Next, we introduce the previously analyzed results [15, 16, 17] for bifurcations of a fixed point observed in reduced models of our system. The reduced models are based on the fact that plural oscillators in an image region can be reduced to an oscillator if we assume that the responses of oscillators in an image region are synchronized in-phase. For example, our system for an image with two image regions is simplified as a model with a global inhibitor and two oscillators without directly excitatory coupling between the oscillators; we call it the two-coupled system. Figure 3 plots the bifurcation sets of a fixed point observed in the two- and three-coupled systems. In the analysis, the values of the system parameters except for k_r and ϕ were set to $k_f = 0.5$, $d_1 = d_2 = 2$, $W_z = 15$, $\theta_z = 0.5$, $W_x = 15$, $\theta_c = 0$, $\alpha = 4$, $a = 0.5$, $\theta_f = 15$, $\theta_d = 0$, and $\varepsilon = 0.1$. The NS_ℓ^1 denotes a Neimark-Sacker bifurcation curve of the fixed point, where the subscript number ℓ was appended to distinguish between bifurcation sets of the same type. The stable fixed point exists only in the shaded parameter region and is destabilized at the Neimark-Sacker bifurcation points. Multiple Neimark-Sacker bifurcations occur at parameter values on the curve NS_1^1 . For example, in the two-coupled system, the number of characteristic multipliers that are outside of the unit circle is changed from 0 to 4 when the value of k_r passes through the curve NS_1^1 from the inside to the outside of the shaded region; in the three-coupled system, its number is changed from 0 to 6.

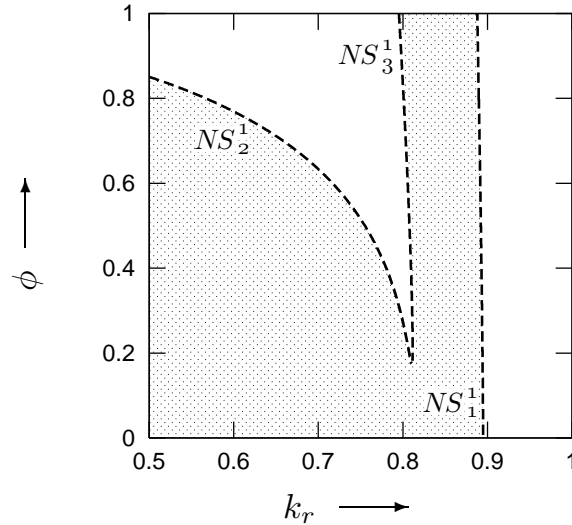


FIGURE 3. Bifurcation diagram of a fixed point observed in reduced model [15, 16, 17]

4. Experimental Results and Discussion. Let us consider the relevance between the arrangement of characteristic multipliers of a fixed point when it bifurcates and the number of image regions in an input image. To simplify the problem, we treated only binary (black and white) images, shown in Figures 4(a)-4(c). The dimension numbers in our system to segment 2×2 , 3×3 , and 20×20 images are 9, 19, and 801, respectively. Here, so that double Neimark-Sacker bifurcations of a stable fixed point can occur, we set $k_r = 0.88974207$ and $\phi = 0.8$ that correspond to a near point at NS_1^1 in Figure 3. We also set $d_i = 2$ and $d_j = 0$ in the i th and j th oscillators corresponding to white and black pixels, respectively. The values of the other parameters were set to the values described in Section 3. Note that because the occurrence of bifurcations is sensitive to the change of parameter values, the parameter values should be set to the bifurcation point as accurately as possible.

First, in our system for the 2×2 image with two white image regions and two black pixels, we found a fixed point $\mathbf{x}^* = (32.096, -31.565, -1.756, 1.516, -1.756, 1.516, 32.096, -31.565, 0.222)^\top$ at the parameter values; its characteristic multipliers were $(0.5, 0.5, -0.8, 0.964 - 0.266i, 0.964 + 0.266i, 0.964 + 0.266i, 0.964 - 0.266i, -2.162, -2.162)^\top$. The numbers of characteristic multipliers inside and outside of a unit circle in the complex plane are three and two, respectively. The four residual ones consist of two pairs of complex conjugates on the circumference of the unit circle (i.e., those that caused the double

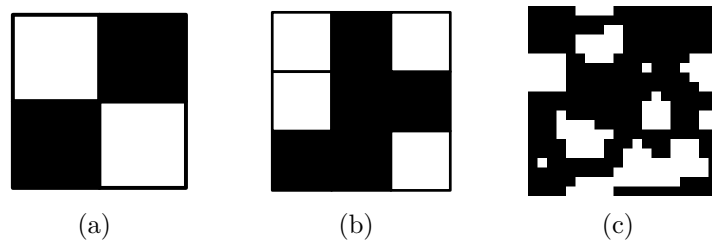


FIGURE 4. Black and white images: (a) 2×2 pixels with two white image regions, (b) 3×3 pixels with three white image regions, and (c) 20×20 pixels with 10 white image regions

Neimark-Sacker bifurcations), which makes this consistent with the analyzed results of the two-coupled system [15, 17]. Figure 5(a) plots the characteristic multipliers on the inside, left outside, and circumference of the unit circle as black, red, and blue points, respectively. Note that some points overlap.

Second, we found a fixed point in our system for the 3×3 image with three white image regions and five black pixels, which can be reduced to a three-coupled system. The characteristic multipliers of the fixed point were $(0.5, 0.5, 0.5, 0.5, 0.5, 0.5, 0.694, -0.8, 0.964 - 0.266i, 0.964 + 0.266i, 0.964 - 0.266i, 0.964 + 0.266i, 0.964 - 0.266i, 0.964 + 0.266i, -2.162, -2.162, -2.162, -2.162, -2.162)^\top$ and are plotted in Figure 5(b). The numbers of characteristic multipliers on the inside, outside, and circumference of the unit circle in the complex plane are 8, 5, and 6, respectively. These three pairs of complex-conjugate characteristic multipliers give rise to triple Neimark-Sacker bifurcations, which is also consistent with the analyzed results of the three-coupled system [16, 17].

The results lead us to the following hypotheses.

1. The number of pairs of complex-conjugate characteristic multipliers that cause multiple Neimark-Sacker bifurcations is equal to the number of image regions.

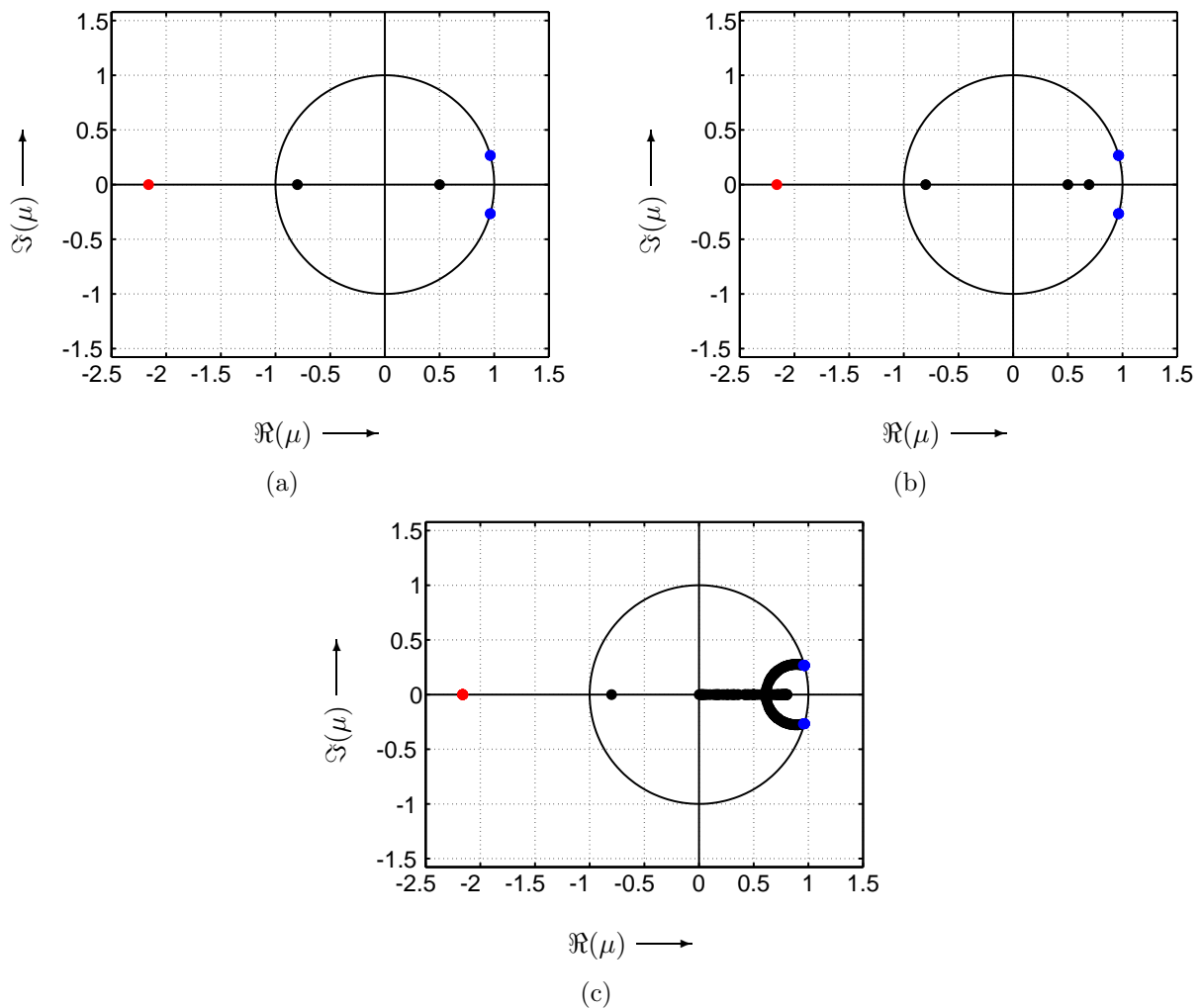


FIGURE 5. Arrangement of characteristic multipliers of a fixed point in proposed system for (a) 2×2 image, (b) 3×3 image, and (c) 20×20 image. \Re and \Im correspond to the real and imaginary part of the complex number.

2. The number of characteristic multipliers arranged on $(-\infty, -1)$ is equal to the number of black pixels corresponding to background regions.
3. The other characteristic multipliers are arranged inside of a unit circle.

In other words, if we compute the number of pairs of complex-conjugate characteristic multipliers that cause multiple Neimark-Sacker bifurcations of a fixed point, we can identify the number of image regions to be segmented in a given binary image.

To test the hypotheses, we computed a fixed point and its characteristic multipliers in our system for the 20×20 image with 10 white image regions and 273 black pixels; the characteristic multipliers are plotted in Figure 5(c). Results showed that the number of characteristic multipliers arranged on the left outside of the unit circle was 273 and corresponded to the number of black pixels, and the pairs of complex-conjugate characteristic multipliers was 10, which corresponded to the white image regions. Through our other experiments for input images with the different number and shape of image regions, we confirmed that the locations of fixed points and their bifurcation points were almost unchanged at the same parameter values, i.e., the differences of their locations were negligibly small. These demonstrate that our hypothesis is effective and suggest that our method to identify the number of image regions to be segmented in a given binary image is also effective. However, it is difficult to apply our method to large images. Its feasibility for large images depends on the performance of computers and an algorithm to compute eigenvalues of a large matrix.

5. Conclusion. We considered the relevance between the number of image regions to be segmented in a given binary image and the arrangement of the characteristic multipliers of a fixed point when the system bifurcates. The results showed that the number of image regions is the same as the number of characteristic multipliers that cause multiple Neimark-Sacker bifurcations of a fixed point. This demonstrates the suitability of our method to identify the number of image regions. Note that our approach is also applicable to gray-scale images and color images using a discrete-time multi-scaling system [20] that makes the degradation (posterization) of a given image as pre-processing.

Acknowledgment. This research was partially supported by KAKENHI (#22700234) and the Aihara Innovative Mathematical Modelling Project, the Japan Society for the Promotion of Science (JSPS) through the “Funding Program for World-Leading Innovative R&D on Science and Technology (FIRST Program),” initiated by the Council for Science and Technology Policy (CSTP).

REFERENCES

- [1] A. Pikovsky, M. Rosenblum and J. Kurths, *Synchronization: A Universal Concept in Nonlinear Sciences*, Cambridge University Press, Cambridge, 2003.
- [2] G. V. Osipov, J. Kurths and C. Zhou, *Synchronization in Oscillatory Networks*, Springer, Heidelberg, 2007.
- [3] C. Chen, X. Gu, Z. Li, Y. Hu and S. Qiu, Study on impulse synchronization of two arrays coupling with chaotic oscillators, *ICIC Express Letters*, vol.5, no.8(B), pp.2933-2938, 2011.
- [4] Y. Kuramoto, *Chemical Oscillations, Waves, and Turbulence*, Springer-Verlag, 1984.
- [5] D. L. Wang and D. Terman, Locally excitatory globally inhibitory oscillator networks, *IEEE Transactions on Neural Networks*, vol.6, no.1, pp.283-286, 1995.
- [6] D. Terman and D. L. Wang, Global competition and local cooperation in a network of neural oscillators, *Physica D*, vol.81, no.1-2, pp.148-176, 1995.
- [7] S. R. Campbell and D. L. Wang, Synchronization and desynchronization in a network of locally coupled Wilson-Cowan oscillators, *IEEE Transactions on Neural Networks*, vol.7, no.3, pp.541-554, 1996.

- [8] N. R. Pal and S. K. Pal, A review on image segmentation techniques, *Pattern Recognition*, vol.26, no.9, pp.1277-1294, 1993.
- [9] J. C. Russ, *The Image Processing Handbook*, 6th Edition, CRC Press, Florida, 2011.
- [10] C. Zhu, H. Liu, J. Shen, G. Gu, J. Ni and Y. Li, Images segmentation with improved PCNN by differential evolution, *ICIC Express Letters*, vol.5, no.3, pp.713-717, 2011.
- [11] J. A. Hartigan and M. A. Wong, A k -means clustering algorithm, *Journal of the Royal Statistical Society, Series C (Applied Statistics)*, vol.28, no.1, pp.100-108, 1979.
- [12] K. Radhakrishnan and A. C. Hindmarsh, Description and use of LSODE, the Livermore solver for ordinary differential equations, *Lawrence Livermore National Laboratory Report*, vol.UCL-113855, 1993.
- [13] K. Fujimoto, M. Musashi and T. Yoshinaga, Discrete-time dynamic image segmentation system, *Electronics Letters*, vol.44, no.12, pp.727-729, 2008.
- [14] K. Aihara, T. Takabe and M. Toyoda, Chaotic neural networks, *Physics Letters A*, vol.144, no.6-7, pp.333-340, 1990.
- [15] K. Fujimoto, M. Musashi and T. Yoshinaga, Reduced model of discrete-time dynamic image segmentation system and its bifurcation analysis, *International Journal of Imaging Systems and Technology*, vol.19, no.4, pp.283-289, 2009.
- [16] M. Kobayashi, K. Fujimoto and T. Yoshinaga, Bifurcations of oscillatory responses observed in discrete-time coupled neuronal system for dynamic image segmentation, *Journal of Signal Processing*, vol.15, no.2, pp.145-153, 2011.
- [17] K. Fujimoto, M. Kobayashi and T. Yoshinaga, Discrete-time dynamic image-segmentation system, *Discrete Time Systems*, pp.405-424, 2011.
- [18] M. Musashi, K. Fujimoto and T. Yoshinaga, Extraction of image regions using oscillatory responses in chaotic neuronal network, *Proc. of 2010 International Symposium on Nonlinear Theory and Its Applications*, Krakow, pp.169-172, 2010.
- [19] H. Kawakami, Bifurcation of periodic responses in forced dynamic nonlinear circuits: Computation of bifurcation values of the system parameters, *IEEE Transactions on Circuits and Systems*, vol.31, no.3, pp.248-260, 1984.
- [20] L. Zhao, R. A. Furukawa and A. C. Carvalho, A network of coupled chaotic maps for adaptive multi-scale image segmentation, *International Journal of Neural Systems*, vol.13, no.2, pp.129-137, 2003.